ISSN 0005-1179 (print), ISSN 1608-3032 (online), Automation and Remote Control, 2024, Vol. 85, No. 2, pp. 113–133.

NONLINEAR SYSTEMS

On Border-Collision Bifurcations in a Pulse System

Zh. T. Zhusubaliyev[*,a], D. V. Titov[*,b], O. O. Yanochkina[*,c], and U. A. Sopuev[,d]**

[*] *Southwest State University, Kursk, Russia*
[**] *Osh State University, Osh, Kyrgyzstan*
e-mail: [a] *zhanybai@gmail.com,* [b] *amazing2004@inbox.ru,*
[c] *yanoolga@gmail.com,* [d] *ulansopuev@mail.ru*

Received September 26, 2022
Revised December 7, 2023
Accepted December 30, 2023

Abstract—Considering a piecewise smooth map describing the behavior of a pulse-modulated control system, we discuss border-collision related phenomena. We show that in the parameter space which corresponds to the domain of oscillatory mode a mapping is piecewise linear continuous. It is well known that in piecewise linear maps, classical bifurcations, for example, period doubling, tangent, fold bifurcations become degenerate ("degenerate bifurcations"), combining the properties of both smooth and border-collision bifurcations. We found unusual properties of this map, that consist in the fact that border-collision bifurcations of codimension one, including degenerate ones, occur when a pair of points of a periodic orbit simultaneously collides with two switching manifolds. This paper also discuss bifurcations of chaotic attractors such as merging and expansion ("interior") crises, associated with homoclinic bifurcations of unstable periodic orbits.

Keywords: pulse system, differential equations with a discontinuous right-hand side, bimodal piecewise linear mapping, border-collision bifurcations, degenerate bifurcations, merging and expansion bifurcations, chaotic oscillations

DOI: 10.31857/S0005117924020025

1. INTRODUCTION

Let us consider a pulse control system the behavior of which is described by the differential equation with a discontinuous right-hand side [1–8]

$$\frac{T}{T_0}\,\dot{x} + x = f(t,\varphi) - \mu, \quad x \in \mathbb{R}, \tag{1}$$
$$f(t,\varphi) \equiv f(t+1,\varphi), \quad 0 \leqslant \mu < 1, \quad \varphi = q - x(t).$$

Here x is the output of a system [8]; $\dot{x}$ is the derivative of x with respect to t; T_0 is the period of the modulation [8]; T is a time constant; q, μ are parameters; φ and f are the input and output (switching function) signals of the modulator.

Within the time intervals $k < t < k+1$, $k = 0, 1, 2, \ldots$, the function f is determined as [8, 9]:

$$f = \begin{cases} 1, & k \leqslant t \leqslant t_k; \\ 0, & t_k < t < k+1, \end{cases} \tag{2}$$

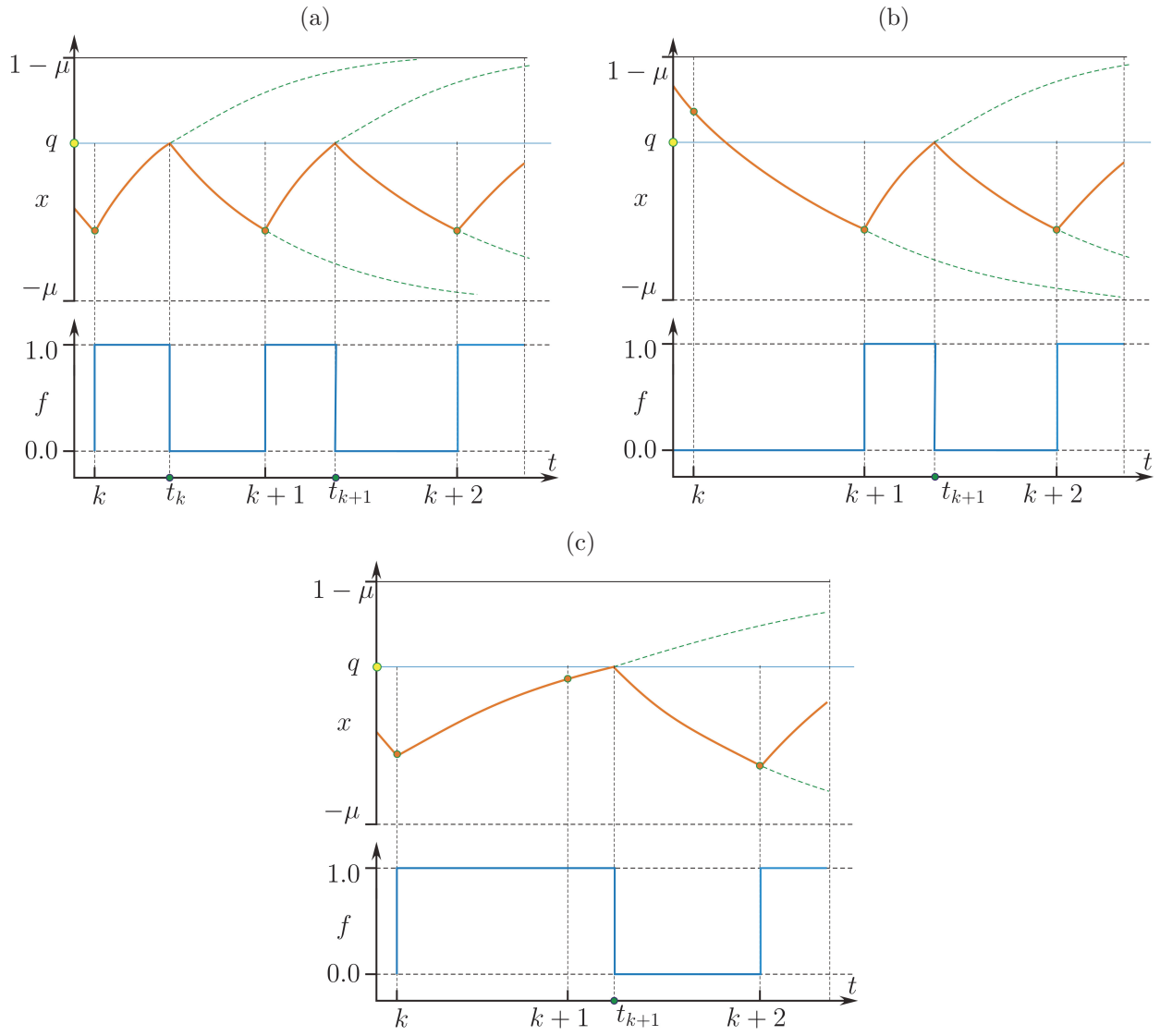

Fig. 1. Generation of the switching signal f. (a) Here t_k is the switching time is determined as $t_k = k + \frac{1}{\lambda}\ln\dfrac{q-1+\mu}{x_k-1+\mu}$, with $x_k = x(t)|_{t=k}$ if $\varphi_k^+ > 0$ and $\varphi_{k+1}^- < 0$. (b) The switching time is equal to $t_k = k$ when $\varphi_k^+ < 0$. (c) The switching time is equal to $t_k = k+1$ if $\varphi_{k+1}^- > 0$.

where t_k is the switching time of the modulator $f = 1 \to f = 0$ (Fig. 1),

$$t_k = \begin{cases} k, & \varphi_k^+ \leqslant 0; \\ t_{k*}, & \varphi_k^+ > 0 \quad \text{and} \quad \varphi_{k+1}^- < 0; \\ k+1, & \varphi_{k+1}^- \geqslant 0, \end{cases} \tag{3}$$

$$\varphi_k^{\pm} = \lim_{t \to k \pm 0} \varphi(t), \quad k \leqslant t_k \leqslant k+1.$$

Here

$$\varphi(t) = q - x(t),$$

where

$$x(t) = 1 - \mu + \mathrm{e}^{\lambda(t-k)}\,(x_k - 1 + \mu), \quad \lambda = -T_0/T$$

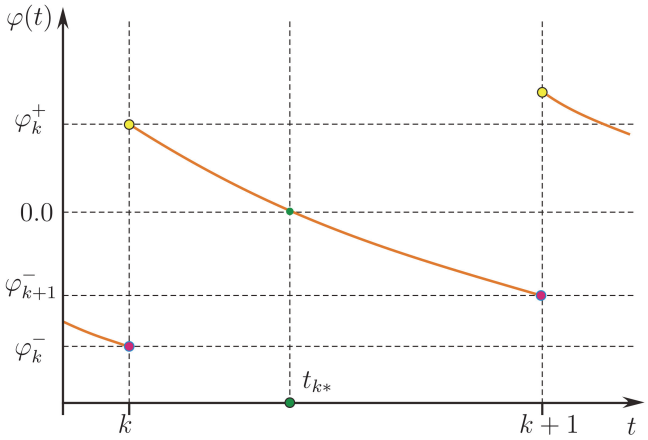

Fig. 2. Function $\varphi(t)$ for the case $\varphi_k^+ > 0$ and $\varphi_{k+1}^- < 0$.

is the solution to (1) when $f = 1$ with an initial condition $x(t)|_{t=k} = x_k$, and t_{k*} is the root of the equation

$$\varphi(t) = q - x(t) = q - 1 + \mu - \mathrm{e}^{\lambda(t-k)} = 0. \tag{4}$$

If $\varphi_k^+ > 0$ and $\varphi_{k+1}^- < 0$ (see Fig. 2), then due to the monotony of $\varphi(t)$ the equation (4) has a single solution

$$t_{k*} = k + \frac{1}{\lambda} \ln \frac{q - 1 + \mu}{x_k - 1 + \mu}, \quad k < t_{k*} < k + 1. \tag{5}$$

If $\varphi_k^+ < 0$ or $\varphi_{k+1}^- > 0$, then equation (4) has no solution. In this case $t_k = k$, if $\varphi_k^+ < 0$, and $t_k = k + 1$, if $\varphi_{k+1}^- > 0$. In both cases, the modulator is saturated.

The period of the periodic solution (1) is a multiple of the period of external action. We will refer to this type of solution as a period-m cycle or m-cycle, $m = 1, \ldots$.

Parameters: $q = 0.356$; $\lambda = -0.6$, $0 < \mu < 1$. Here μ is the control parameter. Figure 3 shows results of numerical experiments, that demonstrate periodic and chaotic solutions (1) for different values of μ.

Figure 3a displays $x(t)$ and the output signal f of the modulator, corresponding to the periodic solution with $m = 1$ $x(t) = x(t + 1)$ for $\mu = 0.18$. Figure 3b demonstrates the period-2 solution of (1) $x(t) = x(t + 2)$ ($\mu = 0.36$). Example of chaotic oscillations ($\mu = 0.4754$) is shown in Fig. 3c.

Figure 3 illustrates a typical property of nonlinear pulse systems [7, 9]. Understanding the mechanisms of the appearance complex behaviors is extremely important for the design, prediction and control dynamics of larger number of control systems [10, 11].

Differential equations of the form (1) may be reduced to the piecewise-smooth mapping $F : I \to I$, $I \subseteq \mathbb{R}$

$$F : x \mapsto F(x) = \begin{cases} F_1(x), & x \in S_1; \\ F_2(x), & x \in S_2; \\ \ldots\ldots & \\ F_p(x), & x \in S_p, \quad p \in \mathbb{N}^+. \end{cases} \tag{6}$$

Here $\mathbb{N}^+$ is the set of strictly positive integers (0 excluded). Each function F_i, $i = 1, \ldots, p$ of (6) is $\mathcal{C}^r$ in its definition S_i.

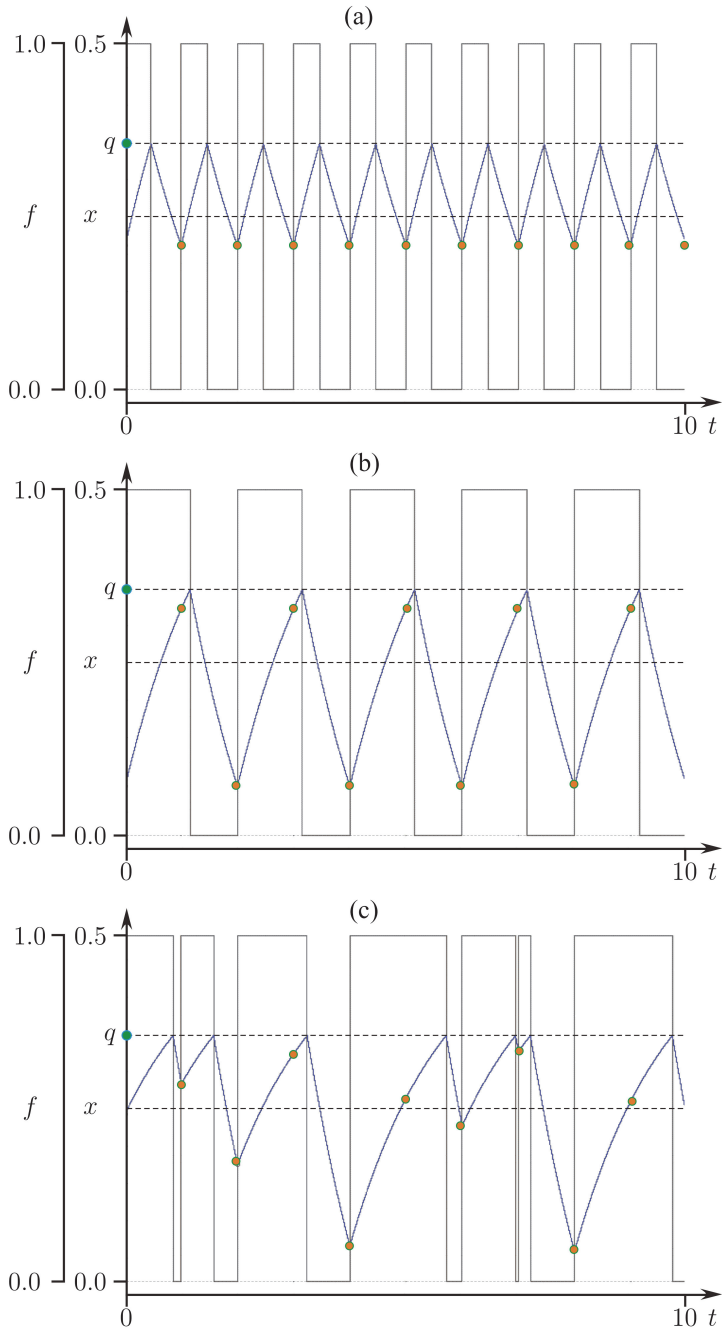

Fig. 3. (a) Periodic oscillations with $m = 1$: $x(t) = x(t+1)$, $\mu = 0.18$. (b) Doubled oscillations: $x(t) = x(t+2)$, $\mu = 0.36$. (c) Chaotic regime, $\mu = 0.4754$.

Note, that $\mathcal{C}^r$, $r > 1$ means that F_i has r derivatives which are continuous at each point of S_i. The borders of S_i are called as switching manifolds.

Fixed points of the map (6) correspond to the periodic solutions of equation (1) with $m = 1$.

Under variation parameters, for example, the fixed/periodic point collides with a switching manifold of F_i. When such a collision causes a change of the topological structure of the phase space of the map, it is called a border-collision bifurcation [12] or "*C-bifurcation*" [13–15].

Border-collision bifurcations have no analogues in smooth dynamical systems and exhibit a special class of nonlinear dynamic phenomena. A simple type of border-collision bifurcations consists

in the direct transition from one periodic orbit into another with the same period. However, more complicated phenomena are also possible, including period-multiplying, multiple-choice bifurcations [16, 17] and direct transition from the fixed or periodic point to chaos [12, 18–25].

Note that border-collision bifurcations are not associated with violation of the hyperbolicity condition of fixed points or cycles, therefore they cannot be described and interpreted by the methods of bifurcation theory for smooth systems [26, 27].

In the present paper, we both numerically and analytically study border collision phenomena in a piecewise smooth mapping obtained from the equation (1). We show that in the parameter space which corresponds to the domain of oscillatory mode a mapping is piecewise linear continuous. It is well known that in piecewise linear maps, classical bifurcations, for example, period doubling, tangent, fold bifurcations become degenerate ("degenerate bifurcations") [25, 28], combining the properties of both smooth and border-collision bifurcations.

We found unusual properties of this map, which consist in the fact that border-collision bifurcations of codimension one, including degenerate ones, occur when a pair of points of a periodic orbit simultaneously collides with two switching manifolds.

The present paper also discuss bifurcations of chaotic attractors such as merging and expansion ("interior") crises, associated with homoclinic bifurcations of unstable periodic orbits [25, 28–31].

In general, it is important to study mechanisms that induce merging and emergence of chaotic attractors. Such phenomena are often called crises [32–34]. There exist three types of crises: merging, boundary and interior crises [32–34]. In this paper we study merging and interior crises.

2. PIECEWISE-SMOOTH MAP

Within the domain $k < t \leqslant t_k$, the function $f = 1$ and the equation (1) has the form

$$\dot{x} = \lambda(x + \mu - 1), \quad x_k = x(t)|_{t=k},$$

with the solution

$$x(t) = \mathrm{e}^{\lambda(t-k)}\,(x_k - 1 + \mu) + 1 - \mu.$$

In this way, at the time $t = t_k$ we have

$$x(t_k) = \mathrm{e}^{\lambda(t_k-k)}\,(x_k - 1 + \mu) + 1 - \mu.$$

In the subsequent time interval $t_k < t < k + 1$, function $f = 0$, and equation (1) takes the form

$$\dot{x} = \lambda\,(x + \mu) - \mu.$$

The solution of this equation with an initial condition

$$x(t_k) = \mathrm{e}^{\lambda(t_k-k)}\,(x_k - 1 + \mu) + 1 - \mu$$

has

$$x(t) = \mathrm{e}^{\lambda(t-k)}\,(x_k - 1 + \mu) - \mu + \mathrm{e}^{\lambda(t-t_k)}.$$

Hence, for $t = k + 1$

$$x_{k+1} = \mathrm{e}^{\lambda}\,(x_k - 1 + \mu) - \mu + \mathrm{e}^{\lambda(k+1-t_k)}. \tag{7}$$

Let's introduce the following notation $z_k = t_k - k$. In this term, the expression (7) can be rewritten in the form:

$$x_{k+1} = F(x_k), \quad F(x) = \mathrm{e}^{\lambda}\,(x - 1 + \mu) - \mu + \mathrm{e}^{\lambda(1-z)}, \tag{8}$$

where z $(0 \leqslant z \leqslant 1)$ is determined as (see (3) and (5)):

$$z = \begin{cases} 0, & q - x \leqslant 0; \\ \dfrac{1}{\lambda}\,\ln\dfrac{q-1+\mu}{x-1+\mu}, & q - x > 0 \quad \text{and} \quad q - 1 + \mu - \mathrm{e}^{\lambda}(x - 1 + \mu) < 0; \\ 1, & q - 1 + \mu - \mathrm{e}^{\lambda}(x - 1 + \mu) \geqslant 0. \end{cases} \tag{9}$$

Here z is the pulse duration [8].

Statement 1. *The function $F(x)$ (8) is piecewise linear. Moreover, if $\mu < 1 - q$, then $F(x)$ is continuous and discontinuous if $\mu > 1 - q$.*

Proof. Let us first show that in the intervals $x \in (-\infty;\ 1 - \mu + (q - 1 + \mu)/\mathrm{e}^{\lambda})$ and $x \in (q\ + \infty)$ the function $F(x)$ is linearly increasing.

Denote $F(x)$ in the specified intervals by $F_{\mathcal{L}}(x)$ and $F_{\mathcal{R}}(x)$ respectively. Find $F_{\mathcal{L}}(x)$ and $F_{\mathcal{R}}(x)$, by substituting the corresponding values z from (9) into the difference equation (8).

Let's write $F(x)$ by substituting the value $z = 1$ into (8)

$$F_{\mathcal{L}}(x) = F(x)|_{z=1} = \mathrm{e}^{\lambda}(x - 1 + \mu) - \mu.$$

The function $F_{\mathcal{L}}(x)$ linearly increasing its domain of definition $(-\infty;\ 1 - \mu + (q - 1 + \mu)/\mathrm{e}^{\lambda})$, since the derivative $F'_{\mathcal{L}}(x)$ is positive: $F'_{\mathcal{L}}(x) = \mathrm{e}^{\lambda} > 0$.

Similarly, we find

$$F_{\mathcal{R}}(x) = F(x)|_{z=0} = \mathrm{e}^{\lambda}(x + \mu) - \mu,$$

which is also linearly increasing on the interval $(q;\ +\infty)$, where it is defined.

It remains to show that on the interval $[1 - \mu + (q - 1 + \mu)/\mathrm{e}^{\lambda};\ q]$ the function $F(x)$ is linearly decreasing. Let's denote it by $F_{\mathcal{M}}(x)$:

$$F_{\mathcal{M}}(x) = \mathrm{e}^{\lambda}\,(x - 1 + \mu) - \mu + \mathrm{e}^{\lambda}/\mathrm{e}^{\lambda\,z}. \tag{10}$$

Let's solve equation (4)

$$q - x(t) = 0,\ x(t) = q - 1 + \mu - \mathrm{e}^{\lambda z}(x_k - 1 + \mu), \quad z = t - k$$

with respect to $\mathrm{e}^{\lambda z}$:

$$\mathrm{e}^{\lambda z} = \frac{q - 1 + m}{x_k - 1 + \mu}. \tag{11}$$

Substituting the resulting expression into (10) and omitting the index k in x_k (see (11)), we get

$$F_{\mathcal{M}}(x) = \frac{q + \mu}{q - 1 + \mu}\,\mathrm{e}^{\lambda}(x - 1 + \mu) - \mu.$$

The domain of definition for the function $F_{\mathcal{M}}(x)$ is the interval $[1 - \mu + (q - 1 + \mu)/\mathrm{e}^{\lambda};\ q]$.

Since $\frac{q+\mu}{q-1+\mu}\,\mathrm{e}^{\lambda} < 0$, then the function $F_{\mathcal{M}}(x)$ is decreasing.

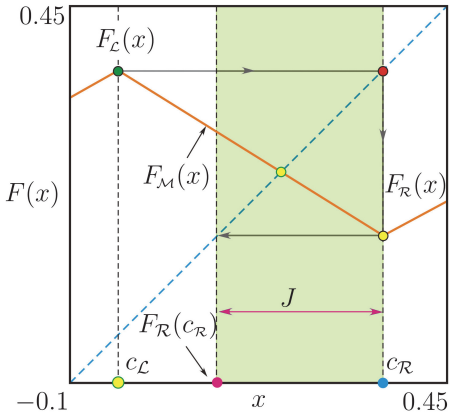

Fig. 4. Bimodal piecewise-linear map.

Let us now prove the continuity of $F(x)$ on the boundaries separating functions $F_{\mathcal{L}}(x)$, $F_{\mathcal{M}}(x)$ and $F_{\mathcal{M}}(x)$, $F_{\mathcal{R}}(x)$. Let's introduce the following notation for the boundaries:

$$c_{\mathcal{L}} = 1 - \mu + \frac{q - 1 + \mu}{\mathrm{e}^{\lambda}}, \quad c_{\mathcal{R}} = q.$$

Since

$$\lim_{x=c_{\mathcal{L}}-0} F(x) = F_{\mathcal{L}}(c_{\mathcal{L}}); \ \lim_{x=c_{\mathcal{L}}+0} F(x) = F_{\mathcal{M}}(c_{\mathcal{L}}), \quad F_{\mathcal{M}}(c_{\mathcal{L}}) = F_{\mathcal{L}}(c_{\mathcal{L}}) = \mathrm{e}^{\lambda}(c_{\mathcal{L}} - 1 + \mu) + 1 - \mu,$$

then the function $F(x)$ is continuous at a point $x = c_{\mathcal{L}}$.

Similarly, it is possible to prove the continuity of the function $F(x)$ at the point $x = c_{\mathcal{R}}$.

It is not difficult to check if $\mu = 1 - q$, then $c_{\mathcal{L}} = c_{\mathcal{R}} = q$.

Hence, in the domain $\mu \geqslant 1 - q$ the function $F(x)$ becomes discontinuity:

$$F(x) = \begin{cases} F_{\mathcal{L}}(x) = \mathrm{e}^{\lambda}(x - 1 + \mu) + 1 - \mu, & x < q; \\ F_{\mathcal{R}}(x) = \mathrm{e}^{\lambda}(x + \mu) - \mu, & x \geqslant q, \end{cases} \qquad (12)$$
$$F_{\mathcal{L}}(q) \neq F_{\mathcal{R}}(q).$$

And so, if $\mu < 1 - q$, then $F(x)$ is noninvertible and contentiously. If then $\mu \geqslant 1 - q$ then $F(x)$ is invertible and discontinuously.

The Statement 1 is proven.

Finally, equation (8) $F : I \to R$, $I \subseteq \mathbb{R}$ can be written in the form

$$F : x \mapsto F(x), \quad F(x) = \begin{cases} F_{\mathcal{L}}(x) = a\,x + b_{\mathcal{L}}, & x < c_{\mathcal{L}}; \\ F_{\mathcal{M}}(x) = a_{\mathcal{M}}\,x + b_{\mathcal{M}}, & c_{\mathcal{L}} \leqslant x \leqslant c_{\mathcal{R}}; \\ F_{\mathcal{R}}(x) = a\,x + b_{\mathcal{R}}, & x > c_{\mathcal{L}}, \end{cases} \qquad (13)$$

where

$$a = \mathrm{e}^{\lambda}, \ b_{\mathcal{L}} = (1 - \mu)\,(1 - \mathrm{e}^{\lambda}), \ b_{\mathcal{R}} = \mu\,(\mathrm{e}^{\lambda} - 1), \ a_{\mathcal{M}} = \frac{q + \mu}{q - 1 + \mu}\,\mathrm{e}^{\lambda},$$
$$b_{\mathcal{M}} = \frac{q + \mu}{q - 1 + \mu}\,\mathrm{e}^{\lambda}\,(\mu - 1) - \mu, \ c_{\mathcal{L}} = 1 - \mu + \frac{q - 1 + \mu}{\mathrm{e}^{\lambda}}, \ c_{\mathcal{R}} = q.$$

Figure 4 illustrates the function $F(x)$. Here the points $c_{\mathcal{L}}$ and $c_{\mathcal{R}}$ are the boundaries, separating the domains of definition of the functions $F_{\mathcal{L}}(x)$, $F_{\mathcal{M}}(x)$ and $F_{\mathcal{R}}(x)$, which are called switching manifolds [21].

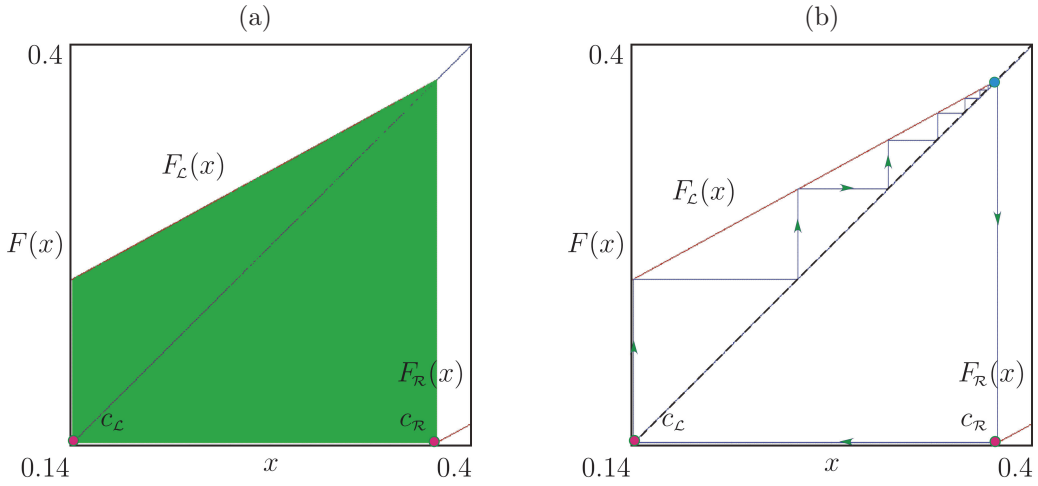

Fig. 5. Discontinuity map.

Note that the discontinuous mapping (12) at $\mu > 1 - q$ has a single stable fixed point

$$F_{\mathcal{L}}(x) - x = 0, \quad F_{\mathcal{L}} = a\,(x - 1 + \mu) + 1 - \mu,$$

corresponding to the equilibrium state of the equation (1): $x - 1 + \mu = 0$ (Fig. 5a). For $\mu = 1 - q$, there is a semi-stable fixed point: on the left it is attractive, and on the right it is repulsive (Fig. 5b). Therefore, the domain of oscillatory mode of the system under consideration is $0 < \mu < 1 - q$.

Before continuing, let's recall the basic concepts [25, 35] and note some of the map (13) properties that will be needed in the future. For to do this, we will rewrite (13) in the equivalent form: $x_{k+1} = F(x_k)$, $k = 0, 1, 2, \ldots$.

- Let us a point $x_0 \in I$, $I \subseteq \mathbb{R}$ is transformed in one iteration by map F into a point $x_1 = F(x_0)$. The point x_1 is called rank-one image of x_0.
- Any point x_0 such that $F(x_0) = x_1$ is a rank-one preimage of x_1, i.e., $x_1 = F^{-1}(x_0)$, where $F^{-1}(x)$ is the inverse function. The rank-k image of a point x_0 is denoted as $F^k(x_0) = F \circ F \circ \ldots \circ F(x_0)$. A rank-$k$ preimage of a point x_0 is a point x which satisfies $F^k(x) = x_0$ or $x = F^{-k}(x_0)$, with $F^{-k}(x_0) = F^{-1} \circ F^{-1} \circ \ldots \circ F^{-1}(x_0)$, $k = 1, 2, \ldots$ (see [35]).
- For any initial point $x_0 \in I$ the map $x_{k+1} = F(x_k)$ is defined a sequence

  $$x_0, F(x_0), F^2(x_0), \ldots, F^k(x_0), \ldots,$$

  which is called a positive orbit $\mathcal{O}^+(x_0)$ of the point x_0:

  $$\mathcal{O}^+(x_0) = \{x_0 \in I : x_0, F^k(x_0), \quad k = 1, 2, \ldots\}.$$

- When defining a negative orbit $\mathcal{O}^-(x_0)$ may be difficult due to the non-invertibility of the map. But if we take all the preimages of x_0, then

  $$\mathcal{O}^-(x_0) = \{x \in I : F^k(x) = x_0, \quad k = 0, 1, 2, \ldots\}.$$

- If

  $$F^m(x_0) - x_0 = 0$$

  in $\mathcal{O}^+(x_0)$ for some $m > 0$, then x_0 is a periodic point. Note that if x_0 is a m-periodic point, then it is km-periodic for any positive integer k [26]. Thus, if m is the smallest positive integer having this property, then m is called the period of a cycle.

- Let's x_0 is the periodic point. Then a finite set of distinguish points

$$\mathcal{O}_m(x_0) = \{x_0 \in I : x_0,\ F^k(x_0),\ k = 1, 2, \ldots, m-1\},$$
$$F^m(x_0) = x_0,\ F^k(x_0) \neq x_0$$

  is called m-periodic cycle or m-cycle. For $m = 1$ we have

$$F(x_0) - x_0 = 0.$$

  Here x_0 is the fixed point or 1-cycle.
  Obviously, the orbit of a fixed point consists of a single point $\mathcal{O}(x_0) = \{x_0\}$ [26].
- If x_0 is the m-periodic point, then it is the fixed point of the function $F^m(x)$ [26].
- A set $E \subseteq I$ is invariant by the map F, if $F(E) = E$. This implies, that if $x \in E$, then $F(x) \in E$. The simplest examples of invariant sets are the fixed points and cycles.
- The m-cycle is (linear) stable, if

$$\rho(\mathcal{O}_m) = \left|\prod_{k=0}^{m-1} F'(x_k)\right| < 1, \quad x_k = F^k(x_0),$$

  where x_k are the periodic points and $\rho(\mathcal{O}_m)$ is the multiplier of the m cycle [26].
- If $\rho(\mathcal{O}_m) \neq 1$, then the m-cycle is called hyperbolic, otherwise it is non-hyperbolic.
- As illustrated in Fig. 4, the function $F(x)$ has two points of local extrema (Fig. 4b): maximum the point $x = c_{\mathcal{L}} = 1 - \mu + \frac{q-1+\mu}{e^{\lambda}}$ minimum at the point $x = c_{\mathcal{R}} = q$. Points of local extrema of the function $F(x)$ are mapped into so-called critical points [25, 35] $c_0 = F_{\mathcal{L}}(c_{\mathcal{L}})$, $c_1 = F_{\mathcal{R}}(c_{\mathcal{R}})$, which are the images rank-1of points $c_{\mathcal{L}}$ and $c_{\mathcal{R}}$ respectively.
- An interval J is said to be absorbing if [25]:
  (a) $F(J) \subseteq J$ i.e. either J is invariant, $F(J) = J$, or it is strictly mapped into itself, $F(J) \subseteq J$);
  (b) there is a neighborhood $\mathcal{U}$ of J such that for any $x \in \mathcal{U}$ there exists a finite integer $k > 0$ such that$F^k(x) \in J$;
  (c) J is bounded by two different critical points, or a critical point and its image.
- As we noted before (see (13) and Fig. 4), we consider a bimodal piecewise-linear continuous map. To describe the orbit of such a mapping we use three characters $\mathcal{L}$, $\mathcal{M}$ and $\mathcal{R}$ ("left", "middle", "right") [25].
  Thus the orbit $\{x_i = F^i(x_0)\}$, $i = 0, 1, 2, \ldots$ is described by a sequence:

$$\sigma_0\sigma_1\sigma_2 \cdots,$$

  where the symbol σ_i, $i = 0, 1, 2, \ldots$ in this sequence for each $i \geqslant 0$ is defined as

$$\sigma_i = \begin{cases} \mathcal{L}, & x_i < c_{\mathcal{L}}; \\ \mathcal{M}, & c_{\mathcal{L}} < x_i < c_{\mathcal{R}}; \\ \mathcal{R}, & x_i > c_{\mathcal{R}}. \end{cases}$$

  For continuous maps it does not matter which symbol is used for the border point, $\mathcal{L}$, $\mathcal{M}$ or $\mathcal{R}$ as the image of this point is uniquely defined [25].
- As is known, in piecewise-smooth systems, different types of periodic motions with the same period are exist. Therefore, to describe m-periodic motion of a different type, we will use the notation $O_{\sigma_0\sigma_1\sigma_2\cdots\sigma_{m-1}}$.

Lemma 1. *Let $c_{\mathcal{L}}$ and $c_{\mathcal{R}}$ are the points of local extrema of the function $F(x)$ (13). Then for the critical point $c_0 = F(c_{\mathcal{L}})$ and its pre-image rank-1 following equalities are satisfied*

$$F(c_{\mathcal{L}}) = c_{\mathcal{R}}, \quad F^{-1}(c_{\mathcal{R}}) = c_{\mathcal{L}}, \tag{14}$$

where $F(\cdot) = F_{\mathcal{L}/\mathcal{M}}(\cdot)$.

Proof. The proof of Lemma 1 consists in checking the equalities (14). We first find $F_{\mathcal{L}}^{-1}(x)$ and $F_{\mathcal{M}}^{-1}(x)$:

$$F_{\mathcal{L}}^{-1}(x) = \mathrm{e}^{-\lambda}\,(x - 1 + \mu) + 1 - \mu, \quad F_{\mathcal{M}}^{-1}(x) = \frac{q - 1 + \mu}{(q + \mu)\,\mathrm{e}^{\lambda}}\,(x + \mu) + 1 - \mu. \tag{15}$$

Since $c_{\mathcal{L}} = 1 - \mu + (q - 1 + \mu)/\mathrm{e}^{\lambda}$ and $c_{\mathcal{R}} = q$, then, the expression for $c_{\mathcal{L}}$ and $c_{\mathcal{R}}$ to the left side of the equalities (14), we get

$$F_{\mathcal{L}/\mathcal{M}}(c_{\mathcal{L}}) = q; \quad F_{\mathcal{L}/\mathcal{M}}^{-1}(c_{\mathcal{R}}) = 1 - \mu + (q - 1 + \mu)/\mathrm{e}^{\lambda}.$$

The Lemma 1 has been proved.

This leads to the following statement.

Statement 2. *Let $\mathcal{O}_m$ be a m-cycle (m-periodic orbit). Under variation of the parameters, at least one of the points of the m-periodic orbit $\mathcal{O}_m$ collides with one of the boundaries $c_{\mathcal{L}}$ or $c_{\mathcal{R}}$ (i.e. m-cycle $\mathcal{O}_m$ undergoes border-collision bifurcation), then there is another point lying on the second boundary, so the condition* (14) *is valid for this pair.*

This implies, that in the considered mapping, border-collision bifurcations occur when a pair of points of a periodic orbit $\mathcal{O}_m$ simultaneously collides with two switching manifolds. Thus, at the bifurcation point we have a periodic orbit $\mathcal{O}_m = \{x_0, F(x_0), F^2(x_0), \ldots, F^{m-1}(x_0)\}$, $F^m(x_0) - x_0 = 0$, $x_0 = c_{\mathcal{L}}$, $F(x_0) = c_{\mathcal{R}}$, which can be hyperbolic or non-hyperbolic (in the case of a degenerate bifurcation).

3. BIFURCATION ANALYSIS AND NUMERICAL EXPERIMENTS

In the domain of oscillatory dynamics the map (13) has a single fixed point $O_{\mathcal{M}} = \{x_*\}$ (1-cycle), which belongs to the interval $[c_{\mathcal{L}},\ q]$ (Figs. 6a and 6b):

$$x_* = \frac{(q + \mu)\,\mathrm{e}^{\lambda}}{(q + \mu)\,\mathrm{e}^{\lambda} - q + 1 - \mu} - \mu. \tag{16}$$

The stability of this fixed point $O_{\mathcal{M}}$ is determined by the inequality

$$|\rho\,(\mathcal{O}_{\mathcal{M}})\,| < 1, \quad \rho\,(\mathcal{O}_{\mathcal{M}}) = \frac{q + \mu}{q - 1 + \mu}\,\mathrm{e}^{\lambda}.$$

At $\mu = \mu_{\mathrm{Flip}}$ the fixed point $O_{\mathcal{M}}$ undergoes a generate period doubling bifurcation (Fig. 6a and Fig. 7a), when

$$\rho\,(\mathcal{O}_{\mathcal{M}}) = \frac{q + \mu}{q - 1 + \mu}\,\mathrm{e}^{\lambda} = -1.$$

Solving this equation with respect to μ, we obtain the bifurcation value of the parameter (the bifurcation point of degenerate bifurcation of doubling the period):

$$\mu_{\mathrm{Flip}}^{1} = \frac{1}{1 + \mathrm{e}^{\lambda}} - q.$$

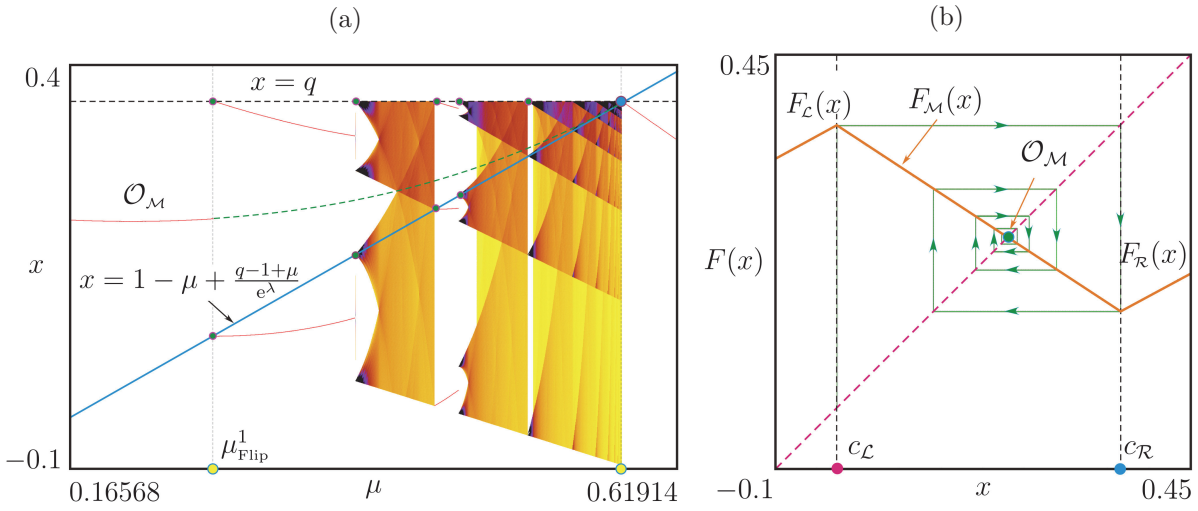

Fig. 6. (a) Bifurcation diagram. (b) Generate period doubling bifurcation of the stable fixed point for $0 < \mu < \dfrac{1}{1+e^\lambda} - q$.

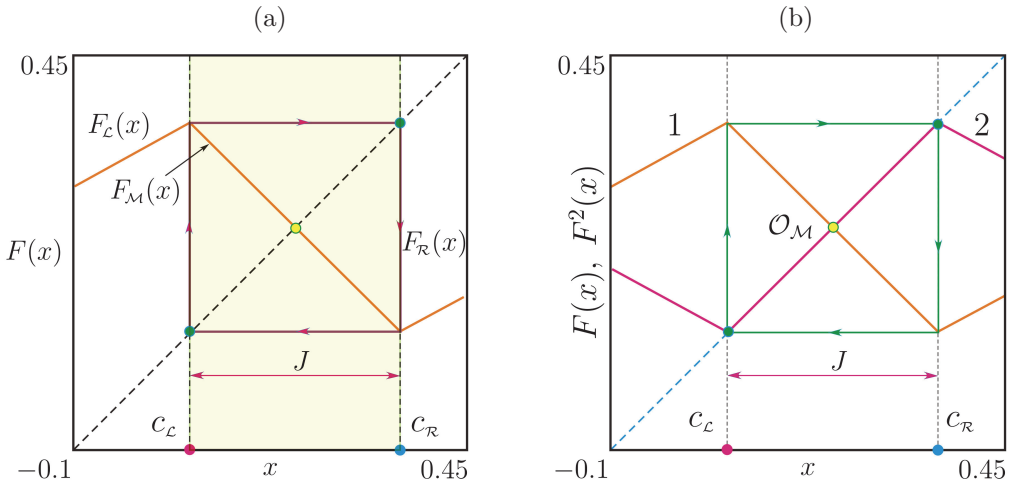

Fig. 7. (a) Generate period doubling bifurcation at the point μ^1_{Flip}. (b) Functions $F(x)$ and $F^2(x)$ at the bifurcation point.

As a result of such a bifurcation, *non-hyperbolic* 2-cycle $\mathcal{O}_2 = \{p_0,\ p_1\}$ arises with multiplier $+1$ (Figs. 7a and 7b), for which

$$F_\mathcal{R} \circ F_\mathcal{L}(c_\mathcal{L}) = c_\mathcal{L}, \quad F_\mathcal{L} \circ F_\mathcal{R}(c_\mathcal{R}) = q.$$

Periodic points p_0, p_1 of the cycle $\mathcal{O}_2$ by virtue of the Lemma 1 (see Fig. 7) are equal to rank-1 critical points $c_0 = F_\mathcal{L}(c_\mathcal{L}) = c_\mathcal{R}$ and $c_1 = F_\mathcal{R}(c_\mathcal{R}) = c_\mathcal{L}$:

$$p_0 = F_\mathcal{R}(c_\mathcal{R}) = q - \frac{1 - e^\lambda}{1 + e^{2\lambda}}, \quad p_1 = F_\mathcal{L}(c_\mathcal{L}) = q.$$

Moreover, any point $x \in J$, $J = [c_\mathcal{L};\ c_\mathcal{R}] = \left[q - \frac{1-e^\lambda}{1+e^\lambda};\ q\right]$, except for $\mathcal{O}_\mathcal{M}$, periodic with period 2.

Indeed (see Fig. 7b), in the interval $J = \left[q - \frac{1-e^\lambda}{1+e^\lambda};\ q\right]$ we have:

$$F(x) = -(x - 1 + \mu) + \mu = -x + 1 \quad \text{and} \quad F^2(x) = x.$$

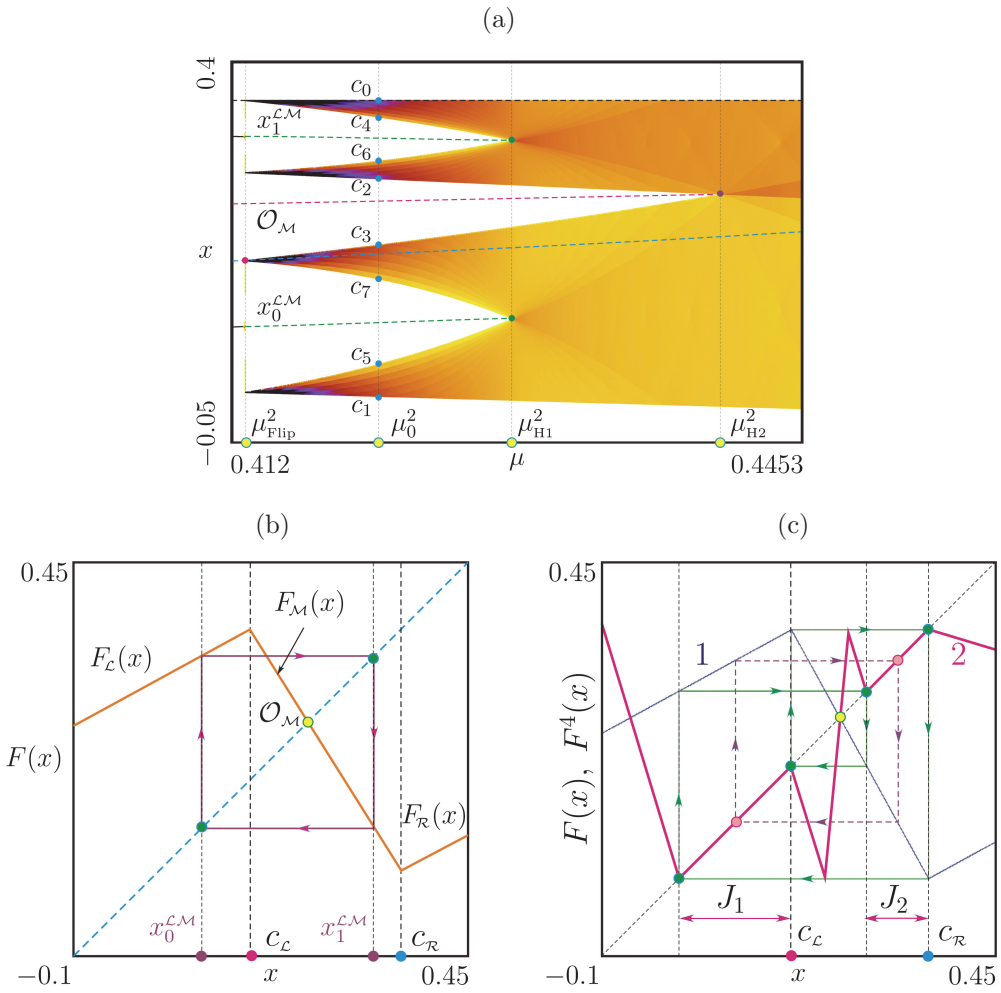

Fig. 8. (a) Bifurcation diagram illustrating a generate period doubling bifurcation for 2-cycle $\mathcal{O}_{\mathcal{LM}}$. (b) The stable 2-cycle $\mathcal{O}_{\mathcal{LM}} = \{x_0^{\mathcal{LM}},\ x_1^{\mathcal{LM}}\}$ in the domain $\mu^1_{\text{Flip}} < \mu < \mu^2_{\text{Flip}}$. (c) Functions $F(x)$ and $F^4(x)$ at the bifurcation point.

From here at the point $\mu = \mu^1_{\text{Flip}}$

$$F\left([F_{\mathcal{M}}(c_{\mathcal{L}});\ q]\right) = [F_{\mathcal{M}}(c_{\mathcal{L}});\ q],$$

where

$$c_{\mathcal{L}} = q - \frac{1 - \mathrm{e}^{\lambda}}{1 + \mathrm{e}^{\lambda}}.$$

When passing the μ parameter through μ^1_{Flip} the fixed point $\mathcal{O}_{\mathcal{M}}$ loses stability, and the non-hyperbolic 2-cycle $\mathcal{O}_2$ becomes stable $\mathcal{O}_{\mathcal{LM}} = \{x_0^{\mathcal{LM}},\ x_1^{\mathcal{LM}}\}$ (see Fig. 8a), where the periodic points are

$$x_0^{\mathcal{LM}} = -\mu + 1 - \frac{\mathrm{e}^{\lambda}\,(q - 1 + \mu)}{q - 1 + \mu - (q + \mu)\mathrm{e}^{2\lambda}},\quad x_1^{\mathcal{LM}} = -\mu - \frac{\mathrm{e}^{2\lambda}\,(q + \mu)}{q - 1 + \mu - (q + \mu)\mathrm{e}^{2\lambda}}.$$

The cycle $\mathcal{O}_{\mathcal{LM}}$ is stable in the interval

$$\frac{1}{1 + \mathrm{e}^{\lambda}} - q < \mu < \frac{1}{1 + \mathrm{e}^{2\lambda}} - q.$$

With a further increase in the parameter, 2-cycle $\mathcal{O}_{\mathcal{LM}}$ (Fig. 8b) undergoes a degenerate period doubling bifurcation. The bifurcation value of the parameter is found from the condition

$$\rho\left(\mathcal{O}_{\mathcal{LM}}\right) = \frac{\mathrm{e}^{2\lambda}\left(q+\mu\right)}{q-1+\mu} = -1.$$

From here we get

$$\mu^2_{\mathrm{Flip}} = \frac{1}{1+\mathrm{e}^{2\lambda}} - q.$$

Such a bifurcation leads to the appearance of a 4-cycle $\mathcal{O}_4$, for which at the point $\mu = \mu^2_{\mathrm{Flip}}$ the condition is valid

$$F_{\mathcal{M}} \circ F_{\mathcal{L}} \circ F_{\mathcal{R}} \circ F_{\mathcal{L}}(c_{\mathcal{L}}) = c_{\mathcal{L}}.$$

As can be seen from Figs. 8b and 8c if $\mu = \mu^2_{\mathrm{Flip}}$, then periodic points p_3, p_4 4-cycles $\mathcal{O}_4 = \{p_0, p_1, p_2, p_3\}$ according to the Lemma 1 lie on switching manifolds $c_{\mathcal{L}}$, $c_{\mathcal{R}}$:

$$p_2 = c_{\mathcal{L}} = \frac{\mathrm{e}^{2\lambda} - \mathrm{e}^{\lambda}}{1+\mathrm{e}^{2\lambda}} + q, \quad p_4 = c_{\mathcal{R}} = q.$$

As in the previous case, all points are $x \in J$, $J = J_1 \bigcup J_2$, except for the periodic points of the 2-cycle $\mathcal{O}_{\mathcal{LM}}$, are periodic with a period of 4 (see Fig. 8b). Here $J_1 = [F_{\mathcal{R}}(q),\ q]$, $J_1 = [F_{\mathcal{L}} \circ F_{\mathcal{R}}(q),\ q]$.

When $\mu > \mu^2_{\mathrm{Flip}}$ from a non-hyperbolic 4-cycle $\mathcal{O}_4$ a four-band chaotic attractor arises (Fig. 9a), which exists in the interval $\mu^2_{\mathrm{Flip}} < \mu < \mu^2_{H1}$ (Fig. 8a). At the point $\mu = \mu^2_{H1}$, the four-band chaotic attractor turns into a two-band one through the so-called "merging bifurcation" associated with homoclinic bifurcation of an unstable 2-cycle $Q_{\mathcal{LM}} = \left\{x_0^{\mathcal{LM}}, x_1^{\mathcal{LM}}\right\}$ (Fig. 8a).

Definition 1. Suppose, a chaotic attractor $\mathcal{A}_k$ consists of k bands, $k > 2$, and there is a repelling m-cycle $\mathcal{O}_m$, $m < k$ with a negative multiplier, located at the boundary of the immediate basin of $\mathcal{A}_k$.

A "merging bifurcation" occurs if at some parameter value the attractor $\mathcal{A}_k$ collides with the cycle $\mathcal{O}_m$ and the bands of the attractor contacting the cycle $\mathcal{O}_m$ merge pairwise [25].

Since the boundaries of a chaotic attractor are formed by critical points and their images, at the bifurcation point the cycle $\mathcal{O}_m$ collides with some of them. This leads to the appearance of a homoclinic orbit to $\mathcal{O}_m$, which is critical at the bifurcation point. As result, the cycle undergoes a homoclinic bifurcation. Being nonhomoclinic before the bifurcation, the cycle necessarily becomes double-side homoclinic after [25, 29].

It is well known that in piecewise smooth continuous maps, when the k-band chaotic attractor $\mathcal{A}_k$, $k = 2m$ undergoes a merging bifurcation, colliding with the m cycle, then all bands merge in pairs, and their number after the merging bifurcation is halved [25, 29].

In Figs. 8a and 9a, 9b shows the transition from a four-band chaotic attractor to a two-band one. An unstable 2-cycle is involved in this transition $\mathcal{O}_{\mathcal{LM}} = \{x_0^{\mathcal{LM}},\ x_1^{\mathcal{LM}}\}$ (see Fig. 8a) with a negative multiplier

$$\rho\left(\mathcal{O}_{\mathcal{LM}}\right) = \frac{\left(q+\mu\right)}{q-1+\mu}\,\mathrm{e}^{2\lambda} < -1.$$

Before bifurcation, the cycle $\mathcal{O}_{\mathcal{LM}}$ is not homoclinic. When increasing μ from the value $\mu^2_{\mathrm{Flip}} = \frac{1}{1+\mathrm{e}^{2\lambda}} - q$ the bands of the attractor $\mathcal{A}_4$ are growing (see Fig. 8a), and then at the point μ^2_{H1}, merge in pairs, colliding with periodic points $x_0^{\mathcal{LM}}$ and $x_1^{\mathcal{LM}}$ (see Fig. 8a).

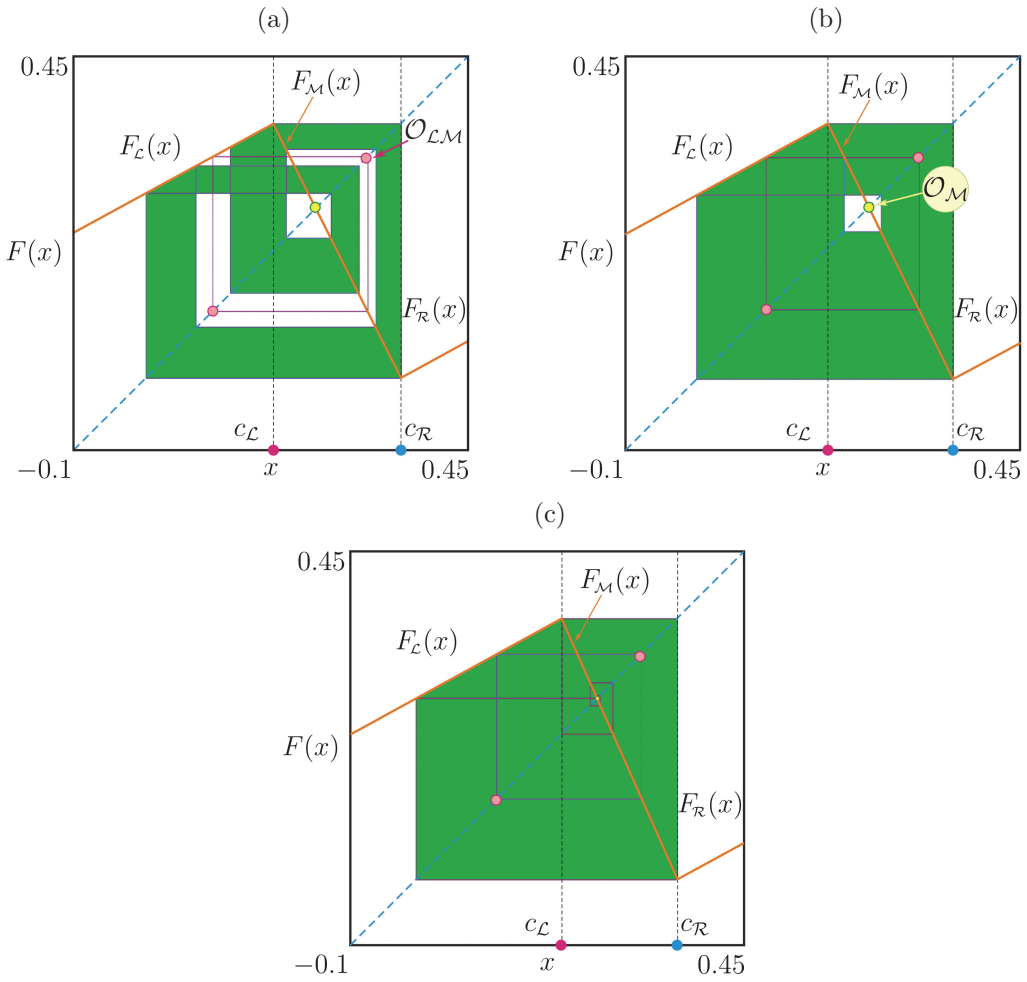

Fig. 9. (a) Four-band chaotic attractor. (b) The transition from a four-band chaotic attractor to a two-band one at the point μ_{H1}^2 in a homoclinic bifurcation of the unstable 2-cycle $\mathcal{O}_{\mathcal{LM}}$. (c) Transition from a two-band chaotic attractor to a single-band one at the point μ_{H2}^2 in a homoclinic bifurcation of the unstable fixed point $\mathcal{O}_{\mathcal{M}}$.

As shown in Fig. 8a (see also Fig. 9b), the upper boundary of the attractor $\mathcal{A}_4$ is equal to $c_0 = q = F_{\mathcal{L}}(c_{\mathcal{L}})$, lower — $c_1 = F_{\mathcal{R}}(q)$. The following boundaries are $c_2 = F_{\mathcal{L}}(c_1)$, $c_3 = F_{\mathcal{L}}(c_2)$, $c_4 = F_{\mathcal{M}}(c_3)$, $c_5 = F_{\mathcal{M}}(c_4)$, $c_6 = F_{\mathcal{L}}(c_7)$ and $c_7 = F_{\mathcal{M}}(c_6)$.

The bifurcation value of the parameter can be found from the condition when the periodic points are $x_0^{\mathcal{LM}}$, $x_1^{\mathcal{LM}}$.

The cycle $\mathcal{O}_{\mathcal{LM}}$ coincide with the critical points defining the corresponding boundaries of the attractor. Thus, the bifurcation value of the parameter can be found by solving any of the equations

$$x_1^{\mathcal{LM}} = c_4, \quad x_1^{\mathcal{LM}} = c_6, \quad x_0^{\mathcal{LM}} = c_5, \quad x_0^{\mathcal{LM}} = c_7.$$

The first equation contains a critical point of the lowest rank. Therefore, it was used to find the bifurcation value of the parameter. This equation has the form

$$\frac{a^4(q+\mu)^3}{(q-1+\mu)^2} - \frac{a^8(q+\mu)^5}{(q-1+\mu)^4} - \frac{a^3(q+\mu)^2}{(q-1+\mu)^2} - \frac{a^6(q+\mu)^4}{(q-1+\mu)^4}$$
$$- \frac{a(q+\mu)}{q-1+\mu} - \frac{a^4(q+\mu)^3}{(q-1+\mu)^3} + \frac{a^2(q+\mu)^3}{q-1+\mu} - 1 + a = 0, \quad a = \mathrm{e}^{\lambda}$$

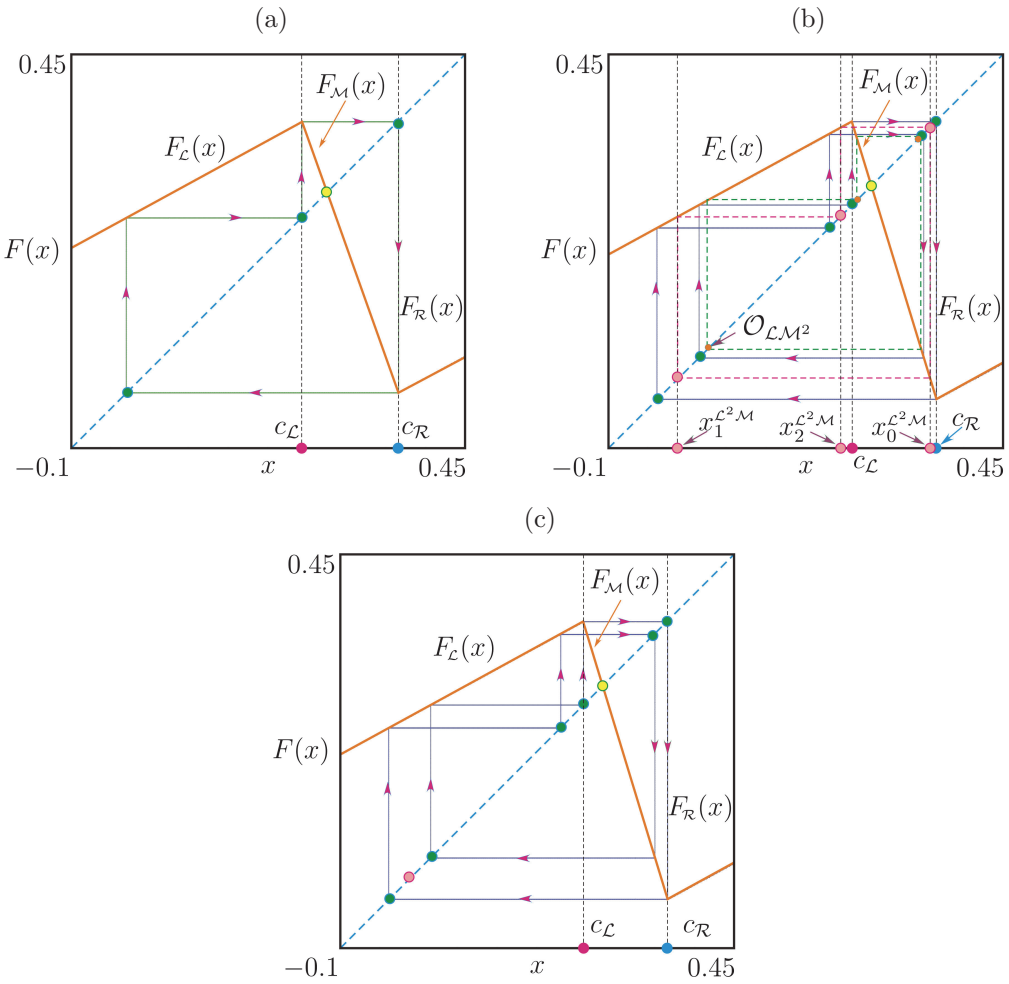

Fig. 10. (a) Non-hyperbolic 3-cycle with a multiplier +1 arising in a border-collision fold bifurcation. (b) Generate period doubling bifurcation for the 3-cycle $O_{\mathcal{L}^2\mathcal{M}}$. (c) Non-hyperbolic 6-cycle arising in a generate period doubling bifurcation.

and solving it numerically with respect to μ, we get μ^2_{H1}.

With a further increase in the parameter, the two-band chaotic $\mathcal{A}_2$ the attractor transforms into a single-band $\mathcal{A}_1$ when at the point μ^2_{H2} (Fig. 8a and Fig. 9b) the bands of the chaotic attractor merge in pairs, colliding with a fixed point $\mathcal{O}_{\mathcal{M}}$. The bifurcation value of the parameter can be found by solving either of the two equations

$$\mathcal{O}_{\mathcal{M}} = c_3, \quad \mathcal{O}_{\mathcal{M}} = c_7.$$

From the first equation we find:

$$\mathrm{e}^{2\lambda}\,(q+\mu)^2 + q + \mu - 1 = 0,$$

whose positive root corresponds to the second point of the merging bifurcation

$$\mu^2_{H2} = -\frac{1}{2\mathrm{e}^{\lambda}}\left(1 - \sqrt{1 + 4\mathrm{e}^{2\lambda}}\right).$$

At the point μ^3_{BCB}, stable and unstable 3-cycles occur in a border-collision bifurcation (Fig. 10a):

$$\mu^3_{\mathrm{BCB}} = \frac{1 - \mathrm{e}^{2\lambda}}{1 - \mathrm{e}^{3\lambda}} - q.$$

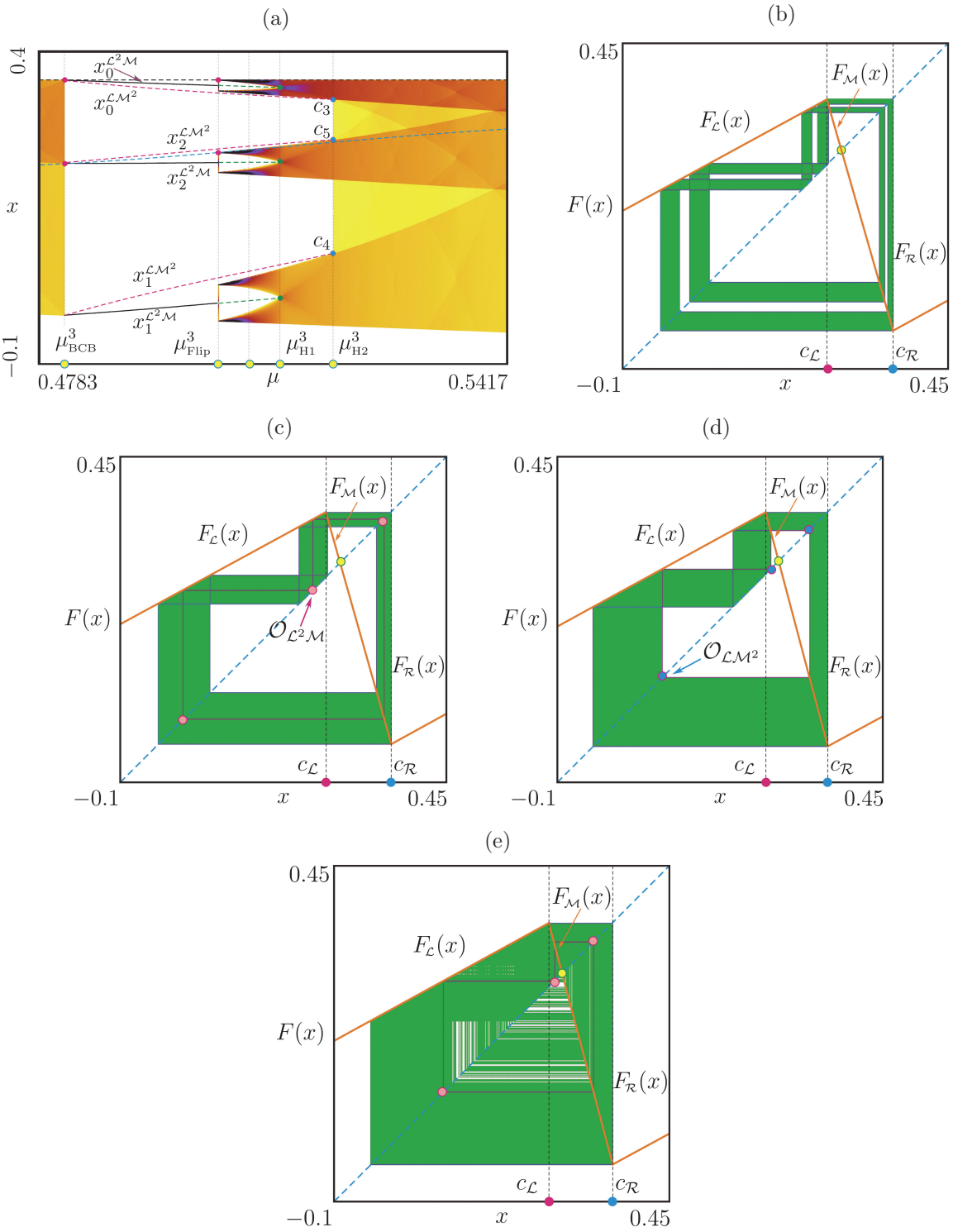

Fig. 11. (a) Bifurcation diagram illustrating merging and expansion bifurcations. (b) Six-band chaotic attractor. (c) Transition from a six-band chaotic attractor to a three-band one at the point μ^3_{H1} in a homoclinic bifurcation of the 3-cycle $\mathcal{O}_{\mathcal{L}^2\mathcal{M}}$. (d), (e) Transition from a three-band chaotic attractor to a single-band one at the point μ^3_{H2} in a homoclinic bifurcation of the unstable 3-cycle $\mathcal{O}_{\mathcal{L}\mathcal{M}^2}$.

With $\mu > \mu^3_{\text{BCB}}$, there are two 3-cycles: stable $\mathcal{O}_{\mathcal{L}^2\mathcal{M}}$ with a negative multiplier and unstable $\mathcal{O}_{\mathcal{L}\mathcal{M}^2}$ with a positive multiplier whose periodic points satisfy the equations

$$F_{\mathcal{L}} \circ F_{\mathcal{L}} \circ F_{\mathcal{M}}(x) - x = 0, \quad F_L \circ F_{\mathcal{M}} \circ F_{\mathcal{M}}(x) - x = 0.$$

Solving these equations, we find $\mathcal{O}_{\mathcal{L}^2\mathcal{M}}$ and $\mathcal{O}_{\mathcal{L}\mathcal{M}^2}$.

The domain of stability for 3-cycle $\mathcal{O}_{\mathcal{L}^2\mathcal{M}}$:

$$\frac{1-\mathrm{e}^{2\lambda}}{1-\mathrm{e}^{3\lambda}} - q < \mu < \frac{1}{1+\mathrm{e}^{3\lambda}} - q.$$

At the point

$$\mu = \mu^3_{\mathrm{Flip}} = \frac{1}{1+\mathrm{e}^{3\lambda}} - q$$

the cycle $\mathcal{O}_{\mathcal{L}^2\mathcal{M}}$ undergoes a degenerate period doubling bifurcation. As in the previous cases, two periodic points of the 6-cycle simultaneously collide with two switching manifolds (Figs. 10b and 10c):

$$F_{\mathcal{L}} \circ F_{\mathcal{M}} \circ F_{\mathcal{L}} \circ F_{\mathcal{L}} \circ F_{\mathcal{R}} \circ F_{\mathcal{L}}(c_{\mathcal{L}}) = c_{\mathcal{L}}.$$

When we pass through μ^3_{Flip} a six-band chaotic attractor appears which in the future is transformed into a three-band attractor in a homoclinic bifurcation (Figs. 11a and 11b). The latter occurs when bands of the chaotic attractor (see Fig. 8a), merge in pairs at the point $\mu = \mu^3_{\mathrm{H1}}$, colliding with periodic points $\{x_0^{\mathcal{L}^2\mathcal{M}}, x_1^{\mathcal{L}^2\mathcal{M}}$ and $x_2^{\mathcal{L}^2\mathcal{M}}\}$ of the unstable 3-cycle $\mathcal{O}_{\mathcal{L}^2\mathcal{M}}$ with negative multiplier

$$\rho\left(\mathcal{O}_{\mathcal{L}^2\mathcal{M}}\right) = \frac{(q+\mu)^3}{(q-1+\mu)^3}\,\mathrm{e}^{3\lambda} < -1.$$

With a further increase in the value parameter μ, at the point μ^3_{H2} so-called an expansion bifurcation [25, 29] (see Figs. 11a and 11c) occurs.

Definition 2. Suppose that the chaotic attractor A_k consists of k bands, $k > 1$, and there is an unstable m-cycle $\mathcal{O}_m$, $m > 1$ with a positive multiplier, located on the boundary of the basin A_k. Expansion bifurcation occurs, when at a certain value of the parameter the attractor $\mathcal{A}_k$ collides with the $\mathcal{O}_m$ cycle and increases dramatically in size [25, 29] .

As in the previous case, such a bifurcation leads to the appearance of a homoclinic orbit for $\mathcal{O}_m$, which is critical at the bifurcation point. The difference is that before bifurcation, the $\mathcal{O}_m$ cycle can be either one-sided homoclinic or non-homoclinic. After bifurcation $\mathcal{O}_m$ becomes two-sided homoclinic [25].

When increasing μ, a three-band chaotic attractor collides with an unstable 3-cycle $O_{\mathcal{L}\mathcal{M}^2}$

$$\rho\left(\mathcal{O}_{\mathcal{L}\mathcal{M}^2}\right) = \frac{(q+\mu)^2}{(q-1+\mu)^2}\,\mathrm{e}^{3\lambda} > 1$$

with a positive multiplier at the point μ^3_{H2}.

As noted above, after bifurcation, the 3-cycle $O_{\mathcal{L}\mathcal{M}^2}$ is a two-sided homoclinic and the chaotic $\mathcal{A}_3$ attractor consists of only one band (Fig. 11e).

As one can be see from Fig. 11a, to calculate the bifurcation point we can use any of the following equations:

$$x_0^{\mathcal{L}\mathcal{M}^2} = c_1, \quad x_1^{\mathcal{L}\mathcal{M}^2} = c_2, \quad x_2^{\mathcal{L}\mathcal{M}^2} = c_4.$$

The first equation contains the image of a critical point of the lowest rank and, therefore, is the simplest to solve. The expansion bifurcation point μ^3_{H2} was found numerically from the equation

$$\frac{a^3(q+\mu)^2 + a^2(q+\mu)(q-1+\mu}{(q-1+\mu)^2 - a^3(q+\mu)^2} = a^3(q+\mu) - a^2 + 1.$$

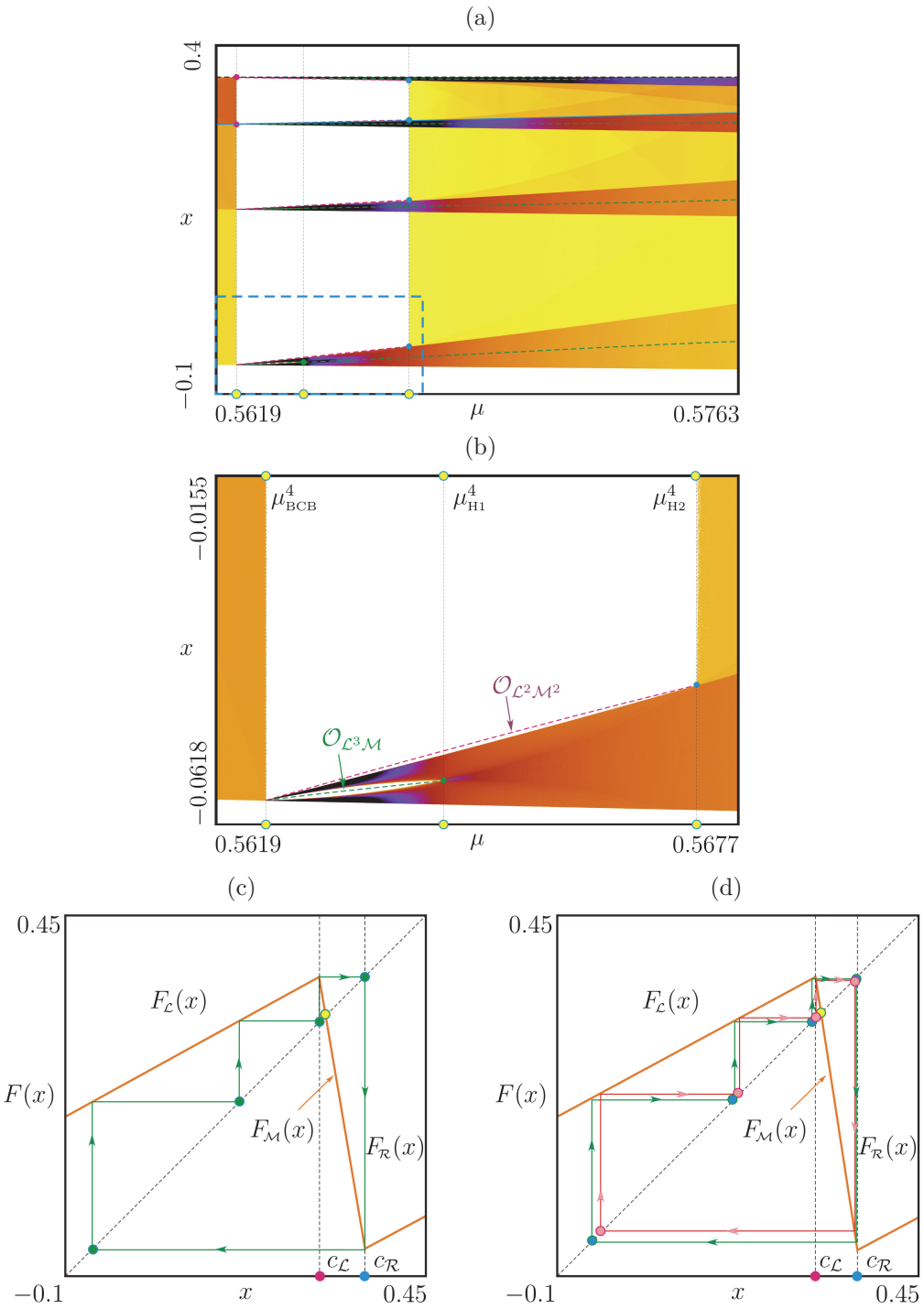

Fig. 12. (a) Bifurcation diagram illustrating merging and expansion bifurcations. (b) Magnified part of the bifurcation is outlined by a dotted rectangle. (c), (d) Appearance of unstable 4-cycles in a border-collision fold bifurcation.

Figure 12 illustrates another transition. At the point μ^4_{BCB} two unstable 4-cycles with a positive and negative multiplier appear (Fig. 12a) in a border-collision bifurcation, when two points of the 4-cycle collide simultaneously with two switching manifolds.

$$\mu^4_{\mathrm{BCB}} = \frac{1-\mathrm{e}^{3\lambda}}{1-\mathrm{e}^{4\lambda}} - q.$$

With an increase in μ, the unstable 4-cycle with a negative multiplier undergoes a merging bifurcation at the point μ^4_{H1}, and an unstable 4-cycle with a positive multiplier undergoes an expansion bifurcation at the point μ^4_{H2} (Fig. 12b).

4. CONCLUSIONS

The purpose of this paper was to present the results of studies of border-collision bifurcations in a piecewise smooth mapping describing the behavior of a pulse control system.

We have shown that such a mapping in the domain of oscillatory dynamics is piecewise linear continuous. It is known that in piecewise linear maps, classical bifurcations, for example, the period doubling bifurcation, tangent and fold bifurcations, become degenerate, combining the properties of both smooth and border-collision bifurcations.

We have found an unusual property of the considered class of pulse systems, which consists in the fact that border -collision bifurcations of codimension one, including degenerate ones, occur when a pair of points of a periodic orbit simultaneously collides with two switching manifolds.

As we know, this case has not been reported before in the general theory of bifurcations of nonsmooth systems. The answer to the question of whether the described phenomenon is related to the property of a particular system remains open.

The second part of the paper was devoted to the study merging and expansion bifurcations [25, 29] of chaotic attractors in pulse systems. This important class of nonlocal bifurcations, also known as crises of chaotic attractors [32–34]) in pulse systems, remains practically unexplored.

Of particular interest are the mechanisms in which the chaotic attractor undergoes sudden changes in sizes. Chaotic attractor may suddenly disappear due to the boundary crisis or suddenly change in size due to the interior crisis (expansion bifurcation) [25, 32–34]. In the present work was studied the merging and interior crisis in the pulse system.

FUNDING

Zh.T. Zhusubaliyev was supported by the Ministry of Education and Science of the Russian Federation within the scope of the “Implementation of the Strategic Academic Leadership program Priority 20302” (1.73.23 П; 1.7.21/S-2): U.A. Sopuev was supported by the Osh State University (grant no. 14-22).

REFERENCES

1. Rozenvasser, E.N., *Periodicheski nestatsionarnye sistemy upravleniya* (Periodic Non-Stationary Control Systems), Moscow: Nauka, 1973.
2. Filippov, A.F., *Differential Equations with Discontinuous Right-hand Sides*, Dortrecht: Kluwer Academic Publishers, 1988.
3. Gelig, A.Kh. and Churilov, A.N., Periodic Modes in Pulse-Width Systems, *Autom. Remote Control*, 1986, vol. 47, no. 11, pp. 1490–1497.
4. Karetnyi, O.Ya. and Kipnis, M.M., Periodic Conditions in Pulse-Width Modulated Control Systems. I, *Avtomatika i Telemekhanika*, 1987, no. 11, pp. 46–54.
5. Karetnyi, O.Ya. and Kipnis, M.M., Periodic Conditions in Pulse-Width Modulated Control Systems. II, *Avtomatika i Telemekhanika*, 1987, no. 12, pp. 42–48.
6. Gelig, A.Kh. and Churilov, A.N., Investigating Ω-Periodic Modes in Pulse-Width Systems, *Autom. Remote Control*, 1989, vol. 50, no. 2, pp. 152–160.
7. Kipnis, M.M., Chaotic Phenomena in a Deterministic One-Dimensional Pulse-Width Control System, *Tekhnicheskaya kibernetika*, 1992, no. 1, pp. 108–112.

8. Gelig, A.Kh. and Churilov, A.N., *Stability and Oscillations of Nonlinear Pulse-Modulated Systems*, Boston: Birkhäuser, 1998.

9. Baushev, V.S. and Zhusubaliyev, Zh.T., On Non-Deterministic Modes of Operation of a Voltage Stabilizer with Pulse-Width Regulation, *Elektrichestvo*, 1992, no. 8, pp. 47–53.

10. Andrievsky, B.R. and Fradkov, A.L., Control of Chaos: Methods and Applications. I. Methods, *Autom. Remote Control*, 2003, vol. 64, no. 5, pp. 673–713.

11. Andrievsky, B.R. and Fradkov, A.L., Control of Chaos: Methods and Aplications. II. Applications, *Autom. Remote Control*, 2004, vol. 65, no. 4, pp. 505–533.

12. Nusse, H.E. and Yorke, J.A., Border-Collision Bifurcations Including "Period Two to Period Three" for Piecewise Smooth Systems, *Physica D*, 1992, vol. 57, no. 1–2, pp. 39–57.

13. Feigin, M.I., Doubling of the Oscillation Period with C-Bifurcations in Piecewise Continuous Systems, *Prikl. Mat. Mekh.*, 1970, vol. 34, no. 5, pp. 861–869.

14. Feigin, M.I., *Vynuzhdennye kolebaniya sistem s razryvnymi nelineinostyami* (Forced Oscillations in Systems with Discontinuous Nonlinearities), Moscow: Nauka, 1994.

15. Di Bernardo, M., Feigin, M.I., Hogan, S.J., and Homer, M.E., Local Analysis of C-bifurcations in n-Dimensional Piecewise-Smooth Dynamical Systems, *Chaos, Solitons and Fractals*, 1999, vol. 19, no. 11, pp. 1881–1908.

16. Kapitaniak, T. and Maistrenko, Yu., Multiple Choice Bifurcations as a Source of Unpredictability in Dynamical Systems, *Phys. Rev. E*, 1998, vol. 58, pp. 5161–5163.

17. Dutta, M., Nusse, H., Ott, R., Yorke, J., and Yuan, G., Multiple Attractor Bifurcations: A Source of Unpredictability in Piecewise Smooth Systems, *Phys. Rev. Lett.*, 1999, vol. 83, pp. 4281–4284.

18. Nordmark, A.B., Non-Periodic Motion Caused by Grazing Incidence in An Impact Oscillator, *J. Sound Vib.*, 1991, vol. 145, pp. 279–297.

19. *Nonlinear Phenomena in Power Electronis*, Banerjee, S. and Verghese, C.C., Eds., New York: IEEE Press, 2001.

20. Zhusubaliyev, Zh.T. and Mosekilde, E., *Bifurcations and Chaos in Piecewise-Smooth Dynamical Systems*, Singapore: World Scientific, 2003.

21. Di Bernardo, M., Budd, C.J., Champneys, A.R., and Kowalczyk, P., *Piecewise-Smooth Dynamical Systems: Theory and Applications*, London: Springer-Verlag, 2008.

22. Di Bernardo, M., Budd, C.J., Champneys, A.R., Kowalczyk, P., Nordmark, A.B., Tost, G.O., and Piiroinen, P.T., Bifurcations in Nonsmooth Dynamical Systems, *SIAM Review*, 2008, vol. 50, pp. 629–701.

23. Avrutin, V., Mosekilde, E., Zhusubaliyev, Zh.T., and Gardini, L., Onset of Chaos in a Single-Phase Power Electronic Inverter, *Chaos*, 2015, no. 25, pp. 043114-1–043114-14.

24. Simpson, D.J.W., Border-Collision Bifurcations in R^N, *SIAM Review*, 2016, vol. 58, pp. 177–226.

25. Avrutin, V., Gardini, L., Sushko, I., and Tramontana, F., *Continuous and Discontinuous Piecewise-Smooth One-Dimensional Maps: Invariant Sets and Bifurcation Structures*, Singapore: World Scientific, 2019.

26. Kuznetsov, Yu.A., *Elements of Applied Bifurcation Theory*, New York: Springer-Verlag, 2004.

27. Shilnikov, L.P., Shilnikov, A.L., Turaev, D.V., and Chua, L.O., *Methods of Qualitative Theory in Nonlinear Dynamics. Parts 1, 2*, Singapore: World Scientific, 1998, 2001.

28. Sushko, I. and Gardini, L., Degenerate Bifurcations and Border Collisions in Piecewise smooth 1D and 2D Maps, *Int. J. Bifurcat. Chaos*, 2010, vol. 20, no. 7, pp. 2045–2070.

29. Avrutin, V., Gardini, L., Schanz, M., and Sushko, I., Bifurcations of Chaotic Attractors in One-Dimensional Maps, *Int. J. Bifurcat. Chaos*, 2014, vol. 24, p. 1440012.

30. Zhusubaliyev, Zh.T., Avrutin, V., and Bastian, F., Transformations of Closed Invariant Curves and Closed-Invariant-Curve-Like Chaotic Attractors in Piecewise Smooth Systems, *Int. J. Bifurcat. Chaos*, 2021, vol. 31, no. 3, p. 2130009.

31. Avrutin, V., Panchuk, A., and Sushko, I., Border Collision Bifurcations of Chaotic Attractors in One-Dimensional Maps with Multiple Discontinuities, *Proc. Roy. Soc. A*, 2021, vol. 477, p. 20210432.

32. Grebogi, C., Ott, E., and Yorke, J.A., Chaotic Attractors in Crisis, *Phys. Rev. Lett.*, 1982, vol. 48, pp. 1507–1510.

33. Grebogi, C., Ott, E., and Yorke, J.A., Crisis: Sudden Changes in Chaotic Attractors and Transient Chaos, *Physica D*, 1983, vol. 7, p. 181.

34. Grebogi, C., Ott, E., Romeiras, F., and Yorke, J.A., Critical Exponents for Crisis-Induced Intermittency, *Phys. Rev. A*, 1987, vol. 36, no. 11, pp. 5365–5380.

35. Mira, C., Gardini, L., Barugola, A., and Cathala, J.C., *Chaotic Dynamics in Two-Dimensional Noninvertible Maps*, Singapore: World Scientific, 1996.

This paper was recommended for publication by A.L. Fradkov, a member of the Editorial Board